Metastatic profiling of HER2-positive breast cancer cell lines in xenograft models

Yuxuan Han[1], Kazushi Azuma[1], Shinya Watanabe[2], Kentaro Semba[1,2], Jun Nakayama[1,3*]

[1] Department of Life Science and Medical Bioscience, School of Advanced Science and Engineering, Waseda University, Tokyo, Japan.

[2] Translational Research Center, Fukushima Medical University, Fukushima, Japan.

[3] Laboratory of Integrative Oncology, National Cancer Center Research Institute, Tokyo, Japan.

[*] Corresponding author

Correspondence to: Jun Nakayama (junakaya@ncc.go.jp, jnakayama.re@gmail.com), Department of Life Science and Medical Bioscience, School of Advanced Science and Engineering, Waseda University, TWIns, 2-2 Wakamatsu-cho, Shinjuku-ku, Tokyo, 162-8480, Japan, Tel/Fax: +81-3-5369-7320.

Keywords: HER2-positive breast cancer; bone metastasis; lung metastasis; in vivo imaging

Abstract

Most studies on breast cancer metastasis have been performed using triple-negative breast cancer (TNBC) cells; thus, subtype-dependent metastatic ability of breast cancer is poorly understood. In this research, we performed intravenous injection (IVI) and intra-caudal arterial injections (CAI) using nine human epidermal growth factor receptor-2 (HER2)-positive breast cancer cell lines for evaluating their metastatic abilities. Our results showed that MDA-MB-453, UACC-893, and HCC-202 had strong bone metastatic abilities, whereas HCC-2218 and HCC-1419 did not show bone metastasis. HER2-positive cell lines could hardly metastasize to the lung through IVI. From the genomic analysis, gene signatures were extracted according to the breast cancer subtypes and their metastatic preferences. The UACC-893 cell line was identified as a useful model for the metastasis study of HER2-positive breast cancer. Combined with

our previous result on brain proliferation ability, we provide a characteristic metastasis profile of HER2-positive breast cancer cell lines in this study.

Statements and Declarations

Acknowledgments

We thank Ms Yuka Kuroiwa and laboratory members for the meaningful comments and discussion.

Funding

This study was supported by JSPS KAKENHI (grant no. 18K16269: Grant-in-Aid for Early-Career Scientist to J.N.; grant no. 20J01794, Grant-in-Aid for JSPS fellows to J.N.; grant no. 20J23297, Grant-in-Aid for JSPS fellows to Y.H.) and partially supported by the grants for translational research programs from Fukushima Prefecture (S.W. and K.S.).

Authorship

YH and KA performed the *in vivo* experiments and bioinformatical analyses. SW, and KS interpreted the data. YH, KA, and JN wrote the manuscript. JN conceived and designed the study. All the authors reviewed and edited the manuscript.

Competing Interests

The authors declare that they have no competing interests.

Ethical approval

The animal experiments were conducted under the approval of the ethics committee of Waseda University (2020-A067, 2021-A074).

Introduction

Breast cancer is the most frequently diagnosed cancer worldwide and appears as the leading cause of cancer death in females [1]. Cancer cell lines derived from human tumors are widely used in metastasis study for their potential usefulness in evaluating preclinical trials [2]. Triple-negative subtype MDA-MB-231 cells and luminal-A subtype MCF7 cells have been most frequently studied in breast cancer metastasis. A recent study that used intracardiac transplantation released a large-scale metastasis map (MetMap500) of human cancer cell lines [3]. The work provided a large-scale characterization of human cancer cell lines and the tool to examine their molecular mechanisms in organ-specific microenvironments. However, their metastasis map was mainly constructed using the groups of luminal and triple-negative cell lines in breast cancer. The metastatic potentials of HER2-positive breast cancer cell lines remain unclear.

HER2 is overexpressed in 20% of breast cancers, and HER2-positive breast cancer is known to be aggressive and have poor outcomes [4]. Although treatments targeting HER2 by chemotherapy and trastuzumab therapy has been well developed, approximately 25% of patients still experience a relapse in distant metastatic organs [5, 6]. Thus, the molecular mechanisms of metastasis in HER2-positive breast cancer must be understood, and the therapeutic strategies for metastasis should be established. However, only few *in vivo* metastasis models of HER2-positive breast cancer are available for the study of their metastatic mechanisms. The *in vivo* transplantation methods affect the evaluation of metastatic potentials and extracted metastasis gene signatures from human cancer cell lines [7]. Therefore, not only intracardiac injection, but also various transplantation methods must be used to evaluate metastatic activities.

In our previous research, we transplanted nine HER2-positive breast cancer cell lines in the brain using intracranial injection and classified them into two groups according to their proliferation abilities in the brain [8]. In this study, we evaluated the lung and bone metastatic potentials of the nine HER2-positive breast cancer cell lines by intravenous injection (IVI) and intracaudal arterial injection (CAI). As a result, the HER2-postive cell lines were classified according to their metastasis abilities. Furthermore, an expression analysis of the cell lines identified the cancer subtype and organ-specific gene signatures.

Materials and Methods

Cell culture

MDA-MB-453, UACC-893, HCC-2218, HCC-1419 (ATCC, Manassas, VA, USA), and ZR-75-1 cells (Institute of Development, Aging and Cancer [IDAC], Miyagi, Japan) were cultured in Roswell Park Memorial Institute medium (RPMI-1640, Fujifilm Wako Pure Chemical Corporation, Osaka, Japan) supplemented with 10% fetal bovine serum (FBS; Nichirei Biosciences Inc., Tokyo, Japan), 100 U/mL penicillin (Meiji-Seika Pharma Co., Ltd., Tokyo, Japan), and 100 µg/mL streptomycin (Meiji-Seika Pharma), and incubated under 37°C with 5% CO_2. MDA-MB-361 and HCC-202 cells (ATCC) were cultured in RPMI-1640 supplemented with 15% heat-inactivated FBS, 100 U/mL penicillin, and 100 µg/mL streptomycin at 37°C with 5% CO_2. BT-474 and UACC-812 (ATCC) were cultured in Dulbecco's modified Eagle's medium (Fujifilm Wako Pure Chemical Corporation) supplemented with 10% heat-inactivated FBS, 15% glucose, 100 U/mL penicillin (Meiji Seika Pharma), and 100 µg/mL streptomycin (Meiji-Seika Pharma) at 37°C with 5% CO_2. UACC-812, MDA-MB-361, HCC-202 cells expressing luciferase were established by infection with lentivirus vector (pLenti-PEF1-*luc2*-IRES-BlaR). UACC-893, MDA-MB-453, HCC-2218, ZR-75-1, BT-474 and HCC-1419 cells were firstly infected with lentivirus vector (pLenti-Pubc-*mSlc7a1*-IRES-HygR) in order to express the ecotropic receptor. These 6 cell lines expressing the ecotropic receptor were infected with retrovirus vector (pMXd3-PEF1-*luc2*-IRES-BlaR). All cell lines and infection protocols were established in a previous study [8].

Animal studies and bioluminescent imaging

Each cell line (5.0×10^5 cells/100 µL phosphate-buffered saline [PBS]) was transplanted into 6-week-old female NOD.CB-17-Prkdc<scid>/J mice (NOD/scid, Charles River Japan, Inc.) via CAI or IVI [9–11]. The mice were anesthetized with 2.5% isoflurane (Fujifilm Wako) during transplantation and bioluminescence imaging (BLI). Bone and lung metastases were monitored using BLI with an IVIS Lumina XRMS In Vivo Imaging System (PerkinElmer) once a week. Each mouse was intraperitoneally injected with 3-mg D-luciferin (Gold

Biotechnology Inc.) in 200-μL PBS before observation. Bioluminescent signal was measured with binning and F/stop ranges suited to each bioluminescence level. The lungs were harvested from the mice at 8 weeks after transplantation. The *ex vivo* observation of the lung was performed using IVIS-XRMS with the D-luciferin solution.

Microarray Analysis

DNA microarray data provided in the previous research were used for genetic analysis [12]. The heatmap was drawn using the "pheatmap" package of R version 3.6.1. The Gene Ontology (GO) term enrichment analysis was performed using Metascape [13]. A principal component analysis (PCA) was performed in R with the "scatterplot3d" package. A Venn diagram was drawn using the "ggplot2" package.

Survival analysis

Survival analysis was performed using the Kaplan-Meier method for patients with breast cancer in the Molecular Taxonomy of Breast Cancer International Consortium (METABRIC) data set, as described previously [8, 14, 15].

Data availability

The microarray data of the nine HER2-positive cell lines were obtained from a previous study [12].

Results

Bone metastasis profiles of the HER2-positive breast cancer cell lines

Nine HER2-positive breast cancer cell lines expressing the *luc2* gene, namely UACC-893, MDA-MB-453, HCC-2218, BT-474, ZR-75-1, UACC-812, MDA-MB-361, HCC-202, and HCC-1419, were transplanted into NOD-SCID mice using the CAI method. After the CAI, MDA-MB-453, UACC-893, and HCC-202 proliferated rapidly at week 8 (Fig. 1a). HCC-2218 and HCC-1419 showed no tumor formation at week 8, which suggests that both have no bone metastatic potential. On the other hand, BT474, ZR-75-1, UACC812, and

MDA-MB-361 migrated and survived in bone microenvironment. Their proliferation abilities were much milder than those of MDA-MB-453, UACC-893, and HCC-202 (Fig. 1b). We further classified the cell lines according to their number of metastasis tumors and proliferation ability into high, medium, low, and not applicable (N/A) groups (Table 1). We noticed that the tumor sizes of HCC-202 and MDA-MB-361 decreased after week 6. This result suggested that HCC-202 and MDA-MB-361 cells might not able to survive in long-term metastasis.

We divided the nine HER2-positive cell lines into two groups. The high metastatic potential group included MDA-MB-453, UACC-893 and HCC-202, and the low/no metastatic potential group included the BT-474, ZR-75-1, UACC-812, MDA-MB-361, HCC-2218, and HCC-1419 cell lines. The gene expression level was standardized into a *z*-score. The genes with average *z*-scores > 1.0 and < −1.0 were counted as upregulated and downregulated genes, respectively (Fig. 2a). We calculated the average log fold-change (FC) ratio change between the high and low potential groups. The genes with an average logFC of >1.0 or 1.0 were counted as differential expression genes (DEGs). Seventy-three upregulated genes and 69 downregulated genes were extracted as gene signatures in HER2-positive breast cancer (Fig. 2b, Table 2). The gene signatures clustered nine breast cancer cell lines into high, medium/low, and N/A metastatic potentials, consistent with our previous data (Table 1). Genes that were reported as metastasis signatures such as tumor-associated calcium signal transducer 2 (*TACSTD2*) and galectin-1 (*LGALS1*) were extracted [16, 17]. Moreover, the metabolisms of amino acids and their derivatives were mostly enriched in the high metastatic group, and the transcriptional regulation of runt-related transcription factor 3 (*RUNX3*) was overall enriched in the high potential group (Fig. 2c). Other than *RUNX3*, nuclear factor-kappa B (*NF-κB*) and metastasis-related runt-related transcription factor 1 (*RUNX1*) signals were also enriched in the high potential groups [18, 19].

Survival analysis of bone gene signatures

To further evaluate the relevance between the extracted gene signatures and the clinical prognosis of patients with HER2-positive breast cancer, we performed a survival analysis

using the METABRIC data set (Fig. 3a, b). The upregulated gene signatures included insulin-induced gene 2 (*INSIG2*), NAD(P)H dehydrogenase, quinone 1 (*NQO1*), and the downregulated gene 4-aminobutyrate aminotransferase (*ABAT*), which correlated with the poor prognosis in HER2-positive breast cancer and all breast cancer subtypes (Supplementary Fig. S1). On the other hand, myotubularin-related protein 2 (*MTMR2*) had HER2-positive-specific clinical signatures that showed no relationship with patient prognosis in all breast cancers. This result also suggests that the clinical markers varied between HER2-positive breast cancer and other breast cancer subtypes.

Lung metastasis profiles of the HER2-positive breast cancer cell lines

Nine cancer cell lines were transplanted into mice via IVI. Slight but substantial luminescence was detected for two cell lines, UACC-893 and HCC-202, which suggests that they have low lung metastasis or viability in the lung (Fig. 4a). However, no luminescence was detected in the other seven cell lines, namely MDA-MB-453, ZR-75-1, HCC-1419, HCC-2218, BT-474, and MDA-MB-361, until week 8 (Fig. 4b). *Ex vivo* BLI was then performed by removing the lungs from each mouse to examine the lung metastatic ability more accurately. In the mice transplanted with UACC-893 and HCC-202, luminescence was detected from the lungs (Fig. 4c). Even *ex vivo* imaging, however, did not detect luminescence from the lungs for the other seven cell lines, namely MDA-MB-453, ZR-75-1, HCC-1419, HCC-2218, BT-474, and MDA-MB-361. On the basis of these results, we classified the UACC-893 and HCC-202 cell lines into a group with low lung metastatic potential, and the remaining seven cell lines into a group without metastasis potential (Table 1).

From the IVI result, we reanalyzed the microarray data using the same strategy as in the reanalysis of data from the group with bone metastasis. The average *z*-score of each gene was calculated for two groups and visualized as a Venn diagram (Fig. 5a). Then, the genes highly or lowly expressed in the low metastasis group only were subjected to GO enrichment analysis. The genes related to lipid metabolism were enriched in the low metastasis group. Next, the genes with an average logFC > 1.0 or −1.0 were extracted as DEGs. In the UACC-893 and HCC-202 cell lines, 162 genes were upregulated, and 95 genes were downregulated as compared with the other seven cell lines (Fig 5b, Table 3). Among the

genes that were highly expressed in UACC-893 and HCC-202 as compared with the no metastasis group are genes such as transmembrane 4 superfamily member 1 (*TM4SF1*) and *LGALS1*. *TM4SF1* was previously reported to promote metastatic activation in multiple organs, including the lung, across breast cancer subtypes [20]. *LGALS1* was previously reported to promote lung metastasis of claudin-low breast cancers [17].

Characterization of HER2-positive cell lines by cancer subtype-specific analysis

To further characterize these HER2-positive cell lines, we clustered the nine HER2-positive cell lines according to their whole-gene expression levels. The nine cell lines were divided into three groups (Fig. 6a). The clustering tree of the HER2-positive cell lines exhibited that the low-lung and high-bone metastasis cell lines UACC-893 and HCC-202 were relevant to each other, while the other HER2-positive cell lines were clustered independently according to their metastatic ability. Next, we quantified their metastasis potential according to their metastatic abilities to each organ site, including the brain metastatic activities and their *in vitro* proliferation ability [8], which has been previously obtained (Table S1). Three dimensional PCA (3D PCA) suggested that the UACC-893 cells had a significant difference in metastatic ability from the rest of the eight cell lines (Fig. 6b).

We previously established the high-metastatic cell lines of luminal breast cancer and triple-negative breast cancer (TNBC) by using the CAI method, and the bone metastasis gene signatures from luminal breast cancer and TNBC proved to be distinct from each other [10]. This suggests that the metastatic mechanism may vary among the molecular subtypes of breast cancer. Therefore, to provide a subtype-specific gene profile of breast cancer, we performed a comparative analysis of the gene signatures between HER2-positive breast cancers, luminal breast cancer, and TNBC (Fig. 7). The result showed no common upregulated or downregulated gene signature among the three subtypes. Six common upregulated signatures were found between luminal and TNBC, and three common upregulated signatures were found between luminal and HER2-positive breast cancers. On the other hand, only one common downregulated gene was found between TNBC and HER2-positive. The common downregulated signature genes both belonged to a family with disintegrin and metalloproteinase with thrombospondin motifs (ADAMTS).

240

241 **Characterization of HER2-positive cell lines by organ-specific analysis**

242 The HER2-positive cell lines exhibited various metastasis characteristics. We compared the
243 extracted gene signatures from bone metastasis, lung metastasis, and brain colorization to
244 demonstrate the organ-specific metastasis features. The results indicated no common
245 upregulated signature among the three organ sites (Fig. 8). However, four common gene
246 signatures, namely 4-aminobutyrate aminotransferase (*ABAT*), MYB proto-oncogene like 1
247 (*MYBL1*), Twist-related protein 1 (*TWIST1*), and olfactomedin 1 (*OLFM1*), were
248 downregulated in the bone, lung, and brain. *ABAT* correlated with the clinical patient
249 prognosis in both HER2-positive breast cancer and all breast cancer subtypes (Fig. 3b,
250 Supplementary Fig S1b). The metastasis signatures of the HER2-positive cells were more
251 commonly shared between bone and lung metastases, rather than brain metastasis. The result
252 of the comparative analysis suggests that brain colonization of HER2-positive breast cancer
253 had a unique mechanism compared with those in bone and lung metastases.

254

255

256 **Discussion**

257 In this study, we established the xenograft models of lung and bone metastases by using nine
258 HER2-positive breast cancer cell lines. Our results profiled their metastatic potentials in
259 xenograft models and provided novel models for future studies on HER2-positive breast
260 cancer metastasis mechanisms.

261 IVIs of UACC-893 and HCC-202 were confirmed to generate weak but significant
262 luminescence in the lung. Thus, they can proliferate very slowly or continue to survive
263 without proliferation. The enrichment analysis revealed that genes involved in lipid
264 metabolism were enriched in the low metastasis group. Regulation of lipid metabolism
265 contributes to increased aggression of breast cancer [21] and regulation of CSC [22]. In this
266 regard, *PFKFB3* is commonly upregulated as a lipid metabolism-related gene known to be
267 associated with cancer [23]. In addition to *PFKFB3*, *NDRG1* [21], *KDM5B* [24], and
268 *JAK/STAT3* [22] have been reported as lipid metabolism-related genes associated with breast
269 cancer. They may contribute to breast cancer malignancy through cell proliferation, migration,

drug resistance, and cancer stem cells. These two cell lines may be useful for elucidating the new dormancy or survival mechanism in the lungs through the lipid metabolism. The other seven cell lines have no lung metastatic ability. Previous studies reported that IVI has low or no ability to metastasize to the lung in MDA-MB-453 and BT-474 [25]. In addition, by using intracardiac injection method, ZR-75-1 and HCC-1419 have also been reported to have no lung metastatic potential [3]. Other reports indicated that MDA-MB-453 and BT-474 cell lines were able to metastasize to the lung. However, a direct comparison is difficult because the mouse species used for transplantation were different or the number of transplanted cells was extremely large compared with that in this study [26, 27]. Moreover, although IVI was used in this experiment for the purpose of mimicking lung metastasis, previous studies confirmed that the population of enriched cells differs depending on the transplantation method [11]. In fact, one study reported that lung metastasis of the MDA-MB-453 cell line was confirmed by orthotopic transplantation in NSG mice [28]. In this study, we focused on the extravasation abilities and the following colonization and proliferation in the lung, examined using IVI. Thus, different results may be obtained if a pre-metastatic niche induced by orthotopic transplantation plays a significant role in lung metastasis.

From the results of our bone metastasis experiment, three of the nine HER2-positive cell lines, HCC-202, MDA-MB-453, and UACC-893, could rapidly grow in bone microenvironment, whereas the others could hardly form bone metastatic tumor. Even though the metastasis possibility to form a tumor in bone was different among the three cell lines, their high proliferative ability in bone microenvironment during long-term observation demonstrated that they have high bone metastatic ability. Compared with their lung metastatic ability, some of the HER2-positive cell lines exhibited stronger bone metastasis potential and brain colonization ability. Among the nine HER2-positive cell lines, UACC-893 had both lung and bone metastatic potentials and proliferation ability in the brain. This suggests that UACC-893 was a more aggressive cell line than the others and is a suitable model for multiorgan breast cancer metastasis research. As almost no study has focused on UACC-893, our result could contribute to breast cancer metastasis studies.

On the basis of the transcriptome analyses of HER2-positive cell lines, the transcriptional signals of *RUNX3* were enriched in the high bone metastasis group. *RUNX3* was a

downstream effector of the transforming growth factor-β (TGF-β) signal pathway and regulates various cancer-related activities such as epithelial-to-mesenchymal transition (EMT) and cancer cell migration and invasion [29]. TGF-β is crucial in the vicious cycle within bone microenvironment and promotes the osteolytic bone metastasis of breast cancer [30, 31]. Therefore, our finding suggests that *RUNX3* signals may contribute to the vicious cycle between HER2-positive cancer cells and bone microenvironment. On the other hand, the genes that regulated the proteoglycans (PGs) of cancer, including protein kinase B (AKT1) and cell-surface glycoprotein (CD44), were downregulated in the high metastasis potential group. The PGs promote the cell-cell junction and migration ability [32] but can also suppress tumor activities [33]. They may function as tumor metastasis suppressors in HER2-positive cancer bone metastasis.

According to the subtype-specific comparison, the breast cancer subtypes (luminal, HER2, and TNBC) did not share common gene signatures. This suggests that the breast cancer subtypes have unique metastatic mechanisms. The brain colonization abilities of the HER2-positive breast cancer cell lines showed no correlation with HER2 phosphorylation or expression levels [8]. Novel factors in HER2-positive cells could possibly regulate their metastasis preference. From the organ-specific comparison analysis, four common downregulated gene signatures were extracted, including *ABAT*, whose low expression correlated with poor prognosis. *ABAT* is an inhibitory neurotransmitter in the central nervous system. Its high expression level suppressed the lung metastasis ability of MDA-MB-231 [34], and its downregulation is a hallmark of ER+ breast cancer [35]. Downregulation of *ABAT* may also contribute to the multiorgan metastasis of HER2-positive tumor cells.

In conclusion, we classified the nine HER2-positive breast cancer cell lines into metastatic subgroups according to their CAI, IVI, and transcriptomic profiles. The extracted metastasis gene signatures were potential prognostic marker genes of HER2-positive breast cancer. Our results suggest that the UACC-893 cell line is a useful model for breast cancer metastasis studies. These models and gene signatures will contribute to the further understanding of the mechanisms of metastasis in HER2-positive breast cancer.

329 **Reference**

330 1. Jemal A, Bray F, M M, et al (2011) Global cancer statistics. Ca Cancer J Clin
331 61:69–90. https://doi.org/10.3322/caac.20107.
332 2. Liu K, Newbury PA, Glicksberg BS, et al (2019) Evaluating cell lines as models for
333 metastatic breast cancer through integrative analysis of genomic data. Nat Commun
334 10:. https://doi.org/10.1038/s41467-019-10148-6
335 3. Jin X, Demere Z, Nair K, et al (2020) A metastasis map of human cancer cell lines.
336 Nature 588:331–336. https://doi.org/10.1038/s41586-020-2969-2
337 4. Gong Y, Liu YR, Ji P, et al (2017) Impact of molecular subtypes on metastatic breast
338 cancer patients: A SEER population-based study. Sci Rep 7:.
339 https://doi.org/10.1038/srep45411
340 5. Jiang H, Rugo HS (2015) Human epidermal growth factor receptor 2 positive (HER2+)
341 metastatic breast cancer: How the latest results are improving therapeutic options.
342 Ther Adv Med Oncol 7:321–339. https://doi.org/10.1177/1758834015599389
343 6. Asif HM, Sultana S, Ahmed S, et al (2016) HER-2 positive breast cancer - A
344 mini-review. Asian Pacific J Cancer Prev 17:1609–1615.
345 https://doi.org/10.7314/APJCP.2016.17.4.1609
346 7. Nakayama J, Han Y, Kuroiwa Y, et al (2021) The in vivo selection method in breast
347 cancer metastasis. Int J Mol Sci 22:1–19. https://doi.org/10.3390/ijms22041886
348 8. Kuroiwa Y, Nakayama J, Adachi C, et al (2020) Proliferative Classification of
349 Intracranially Injected HER2-positive Breast Cancer Cell Lines. Cancers (Basel) 12:.
350 https://doi.org/10.3390/cancers12071811
351 9. Kuchimaru T, Kataoka N, Nakagawa K, et al (2018) A reliable murine model of bone
352 metastasis by injecting cancer cells through caudal arteries. Nat Commun 9:2981.
353 https://doi.org/10.1038/s41467-018-05366-3
354 10. Han Y, Nakayama J, Hayashi Y, et al (2020) Establishment and characterization of
355 highly osteolytic luminal breast cancer cell lines by intracaudal arterial injection.
356 Genes to Cells 25:111–123. https://doi.org/10.1111/gtc.12743
357 11. Nakayama J, Ito E, Fujimoto J, et al (2017) Comparative analysis of gene regulatory
358 networks of highly metastatic breast cancer cells established by orthotopic

transplantation and intra-circulation injection. Int J Oncol 50:497–504. https://doi.org/10.3892/ijo.2016.3809

12. Ito E, Honma R, Yanagisawa Y, et al (2007) Novel clusters of highly expressed genes accompany genomic amplification in breast cancers. FEBS Lett 581:3909–3914. https://doi.org/10.1016/j.febslet.2007.07.016

13. Zhou Y, Zhou B, Pache L, et al (2019) Metascape provides a biologist-oriented resource for the analysis of systems-level datasets. Nat Commun 10:. https://doi.org/10.1038/s41467-019-09234-6

14. Murakami A, Maekawa M, Kawai K, et al (2019) Cullin-3 / KCTD10 E3 complex is essential for Rac1 activation through RhoB degradation in human epidermal growth factor receptor 2- - positive breast cancer cells. Cancer Sci 110:650–661. https://doi.org/10.1111/cas.13899

15. Nishiyama K, Maekawa M, Nakagita T, et al(2021) CNKSR1 serves as a scaffold to activate an EGFR phosphatase via exclusive interaction with RhoB-GTP. Life Science Alliance. 4:e202101095. doi: 10.26508/lsa.202101095.

16. Goldenberg DM, Stein R, Sharkey RM (2018) The emergence of trophoblast cell-surface antigen 2 (TROP-2) as a novel cancer target. Oncotarget 9:28989–29006. https://doi.org/10.18632/oncotarget.25615

17. Dalotto-Moreno T, Croci DO, Cerliani JP, et al (2013) Targeting galectin-1 overcomes breast cancer-associated immunosuppression and prevents metastatic disease. Cancer Res 73:1107–1117. https://doi.org/10.1158/0008-5472.CAN-12-2418

18. Escárcega RO, Fuentes-Alexandro S, García-Carrasco M, et al (2007) The Transcription Factor Nuclear Factor-kappa B and Cancer. Clin Oncol 19:154–161. https://doi.org/10.1016/j.clon.2006.11.013

19. Li Q, Lai Q, He C, et al (2019) RUNX1 promotes tumour metastasis by activating the Wnt/β-catenin signalling pathway and EMT in colorectal cancer. J Exp Clin Cancer Res 38:. https://doi.org/10.1186/s13046-019-1330-9

20. Hua G, Goutam, Chakraborty Zhanguo Z, Intissar A, et al (2016) Multi-organ Site Metastatic Reactivation Mediated by Non- canonical Discoidin Domain Receptor 1 Signaling. Cell 166:47–62. https://doi.org/10.1016/j.cell.2016.06.009.Multi-organ

21. Sevinsky CJ, Khan F, Kokabee L, et al (2018) NDRG1 regulates neutral lipid metabolism in breast cancer cells. Breast Cancer Res 20:. https://doi.org/10.1186/s13058-018-0980-4

22. Tianyi W, Johannes Francois F, Heehyoung L, et al (2018) JAK/STAT3-Regulated Fatty Acid β-Oxidation Is Critical for Breast Cancer Stem Cell Self-Renewal and Chemoresistance. cell Metab 27:136–150. https://doi.org/10.1016/j.cmet.2017.11.001.JAK/STAT3-Regulated

23. Shi L, Pan H, Liu Z, et al (2017) Roles of PFKFB3 in cancer. Signal Transduct Target Ther 2:. https://doi.org/10.1038/sigtrans.2017.44

24. Zhang ZG, Zhang HS, Sun HL, et al (2019) KDM5B promotes breast cancer cell proliferation and migration via AMPK-mediated lipid metabolism reprogramming. Exp Cell Res 379:182–190. https://doi.org/10.1016/j.yexcr.2019.04.006

25. Clinchy B, Gazdar A, Rabinovsky R, et al (2000) The growth and metastasis of human, HER-2/neu-overexpressing tumor cell lines in male SCID mice. Breast Cancer Res Treat 61:217–228. https://doi.org/10.1023/A:1006494001861

26. Nanni P, Nicoletti G, Palladini A, et al (2012) Multiorgan metastasis of human HER-2+ breast cancer in Rag2-/-;Il2rg-/- mice and treatment with PI3K inhibitor. PLoS One 7:e39626. https://doi.org/10.1371/journal.pone.0039626

27. Hung SW, Chiu CF, Chen TA, et al (2012) Recombinant viral protein VP1 suppresses HER-2 expression and migration/metastasis of breast cancer. Breast Cancer Res Treat 136:89–105. https://doi.org/10.1007/s10549-012-2238-7

28. Cleris, Daidone, Fina, Cappelletti (2019) The Detection and Morphological Analysis of Circulating Tumor and Host Cells in Breast Cancer Xenograft Models. Cells 8:683. https://doi.org/10.3390/cells8070683

29. Chen F, Liu X, Bai J, et al (2016) The emerging role of RUNX3 in cancer metastasis (Review). Oncol Rep 35:1227–1236. https://doi.org/10.3892/or.2015.4515

30. Hiraga T (2019) Bone metastasis: Interaction between cancer cells and bone microenvironment. J Oral Biosci 61:95–98. https://doi.org/10.1016/j.job.2019.02.002

31. Yin JJ, Selander K, Chirgwin JM, et al (1999) TGF-β signaling blockade inhibits PTHrP secretion by breast cancer cells and bone metastases development. J Clin

Invest 103:197–206. https://doi.org/10.1172/JCI3523

32. Barkovskaya A, Buffone A, Žídek M, Weaver VM (2020) Proteoglycans as Mediators of Cancer Tissue Mechanics. Front Cell Dev Biol 8:. https://doi.org/10.3389/fcell.2020.569377

33. Fjeldstad K, Kolset SO (2005) Decreasing the metastatic potential in cancers--targeting the heparan sulfate proteoglycans. Curr Drug Targets 6:665–682. https://doi.org/10.2174/1389450054863662

34. Chen X, Cao Q, Liao R, et al (2019) Loss of ABAT-mediated GABAergic system promotes basal-like breast cancer progression by activating Ca2+-NFAT1 axis. Theranostics 9:34–47. https://doi.org/10.7150/thno.29407

35. Jansen MPHM, Sas L, Sieuwerts AM, et al (2015) Decreased expression of ABAT and STC2 hallmarks ER-positive inflammatory breast cancer and endocrine therapy resistance in advanced disease. Mol Oncol 9:1218–1233. https://doi.org/10.1016/j.molonc.2015.02.006

435 **Figure Legends**

436 **Fig. 1 Intra-caudal arterial injection (CAI) transplantation of HER2-positive cell lines**

437 MDA-MB-453, UACC-893, HCC-202, BT-474, ZR-75-1, UACC-812, MDA-MB-361,
438 HCC-2218, and HCC-1419 cells were injected in NOD/SCID mouse (n = 4) by using the CAI
439 method. The tumor growth was quantified by measuring bioluminescence every week and
440 plotted into a growth curve. Each line showed the corresponding bone metastasis tumor. Left:
441 Bioluminescence on week 1. Right: Bioluminescence on week 8. (a) High bone metastasis
442 potential group. (b) Medium and low bone metastasis potential group.

443

444 **Fig. 2 Extraction of bone metastasis gene signatures of the HER2-positive cell lines**

445 (a) Genes were extracted and further analyzed: logFC < −1 or logFC > 1.0, $p < 0.05$ and FDR
446 < 0.05. The number of upregulated and downregulated genes in the high and low potential
447 groups are summarized in the Venn diagrams. (b) The differential expression gene (DEGs)
448 extracted from the high and low potential groups were analyzed by hierarchical clustering and
449 are shown in a heatmap. (c) The Gene Ontology enrichment analysis of upregulated and
450 downregulated DEGs.

451

452 **Fig. 3 Clinical prognosis of bone metastasis gene signatures**

453 (a) Survival analysis of differential expression gene (DEGs) in the high potential group using
454 the METABRIC data set. The colored region along the curve shows the 95% confidence
455 intervals. The table at the bottom lists the number of patients with high or low gene
456 expression in the HER2-positive subtype. The results of the survival analysis of the
457 upregulated DEGs in the HER2-positive patients are also shown. (b) Survival analysis results
458 of the downregulated DEGs in the HER2-positive patients.

459

460 **Fig. 4. Intravenous injection (IVI) transplantation of the HER2-positive cell lines**

461 UACC-893, HCC-202, MDA-MB-453, ZR-75-1, HCC-1419, HCC-2218, BT-474,
462 MDA-MB-361, and UACC-812 cells were intravenously injected in the NOD-SCID mice
463 (MDA-MB-453, n = 9; UACC-893, n = 7; HCC-202, n = 5; MDA-MB-361, n = 3; others, n =
464 4). Lung metastasis was quantified by measuring bioluminescence every week, and the data

were plotted into a growth curve. Each cell line shows the corresponding mouse. Left: Bioluminescence on week 1. Right: Bioluminescence on week 8. (a) Cell lines in the low metastasis group. (b) Cell lines in the no metastasis group. (c) The lungs were removed from each mouse after the 8-week measurement, and luminescence from the lung was detected using *ex vivo* BLI.

Fig. 5 Extraction of lung metastasis gene signatures of the HER2-positive cell lines

(a) Gene signatures associated with lung metastasis or survival in the low-metastasis group were extracted in the same method as that for gene signatures associated with bone metastasis. The numbers of upregulated and downregulated genes in the low or no metastasis group are shown as Venn diagrams. (b) Differential expression gene (DEGs) between the low and no metastasis groups according to microarray data were analyzed using hierarchical clustering as a heatmap. (c) A Gene Ontology enrichment analysis of the DEGs was performed for the low metastasis group.

Fig. 6 Clustering of metastatic activities in the HER2-positive cell lines

An overview of the metastatic ability of the HER2-positive cell lines is shown. (a) The clustering of whole-gene expression was performed using the wardD2 method. The cell lines were clustered into three groups. (b) The 3-D principal component analysis (PCA) plot of nine HER2-positive breast cancer cell lines according to their metastatic potentials. The PCA was performed as shown in Supplementary Table S1.

Fig. 7 Breast cancer subtype-specific gene signatures in metastasis

The numbers of upregulated and downregulated genes among the luminal, HER2-positive, and TNBC subtypes are summarized as Venn diagrams. The commonly upregulated or downregulated genes are listed in the table at the bottom.

Fig. 8 Organ-specific gene signatures in breast cancer metastasis

The numbers of upregulated and downregulated genes in the bone, lung, and brain are summarized as Venn diagrams. The commonly upregulated or downregulated genes are listed

in the table at the bottom.

Supplementary Figure Legends

Supplementary Fig. S1 Clinical prognosis of bone metastasis gene signatures in all the subtypes

The survival analysis of the DEGs in the high potential group was performed using the METABRIC data set. The table at the bottom lists the number of patients with high or low gene expressions in all the breast cancer subtypes. (a) Survival analysis of the upregulated DEGs in all patients with breast cancer. (b) Survival analysis of the downregulated DEGs in all the patients with breast cancer.

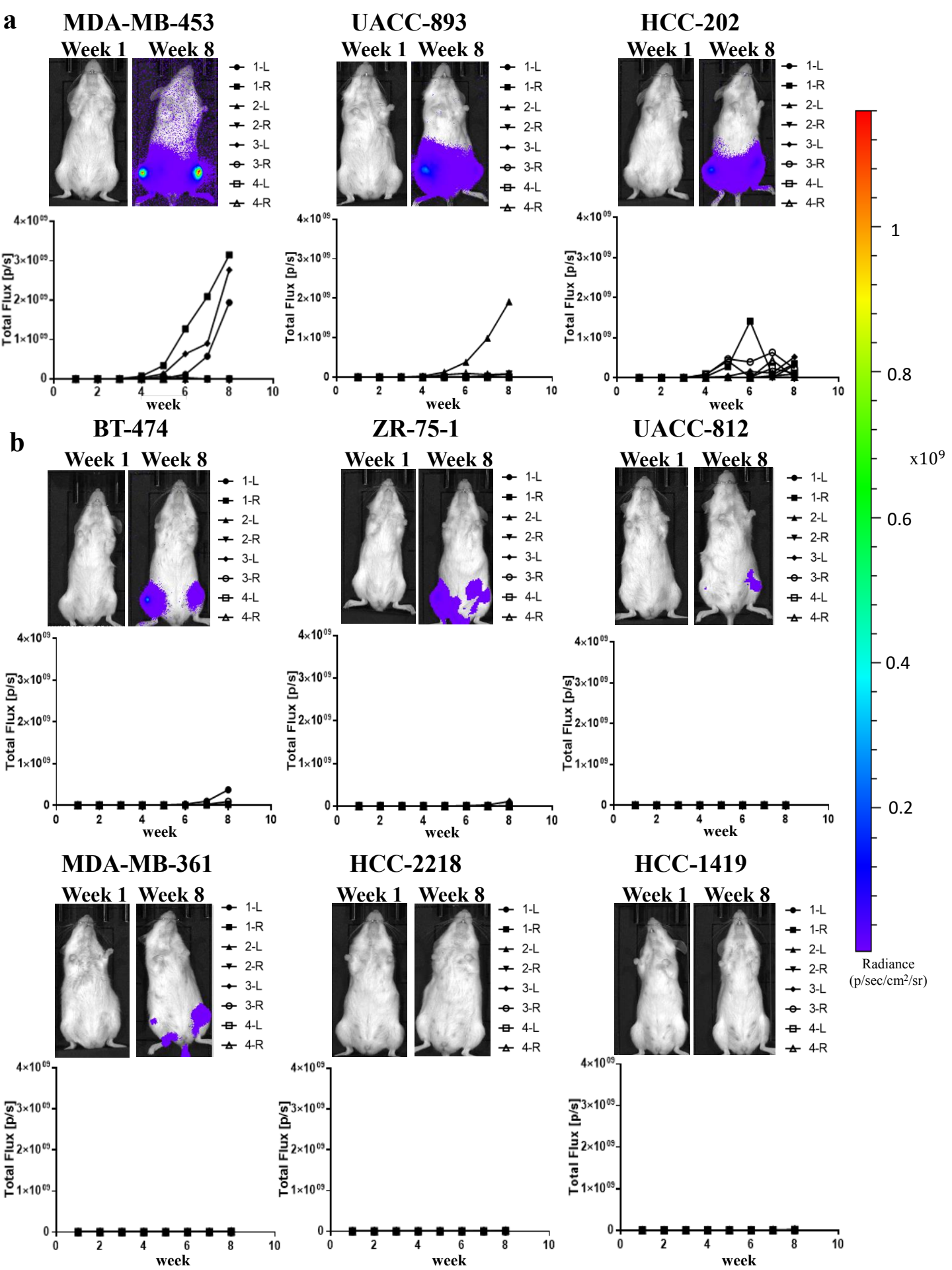
a
MDA-MB-453
UACC-893
HCC-202
b
BT-474
ZR-75-1
UACC-812
MDA-MB-361
HCC-2218
HCC-1419
Week 1
Week 8
1-L
1-R
2-L
2-R
3-L
3-R
4-L
4-R
Total Flux [p/s]
week
Radiance (p/sec/cm²/sr)
x10⁹

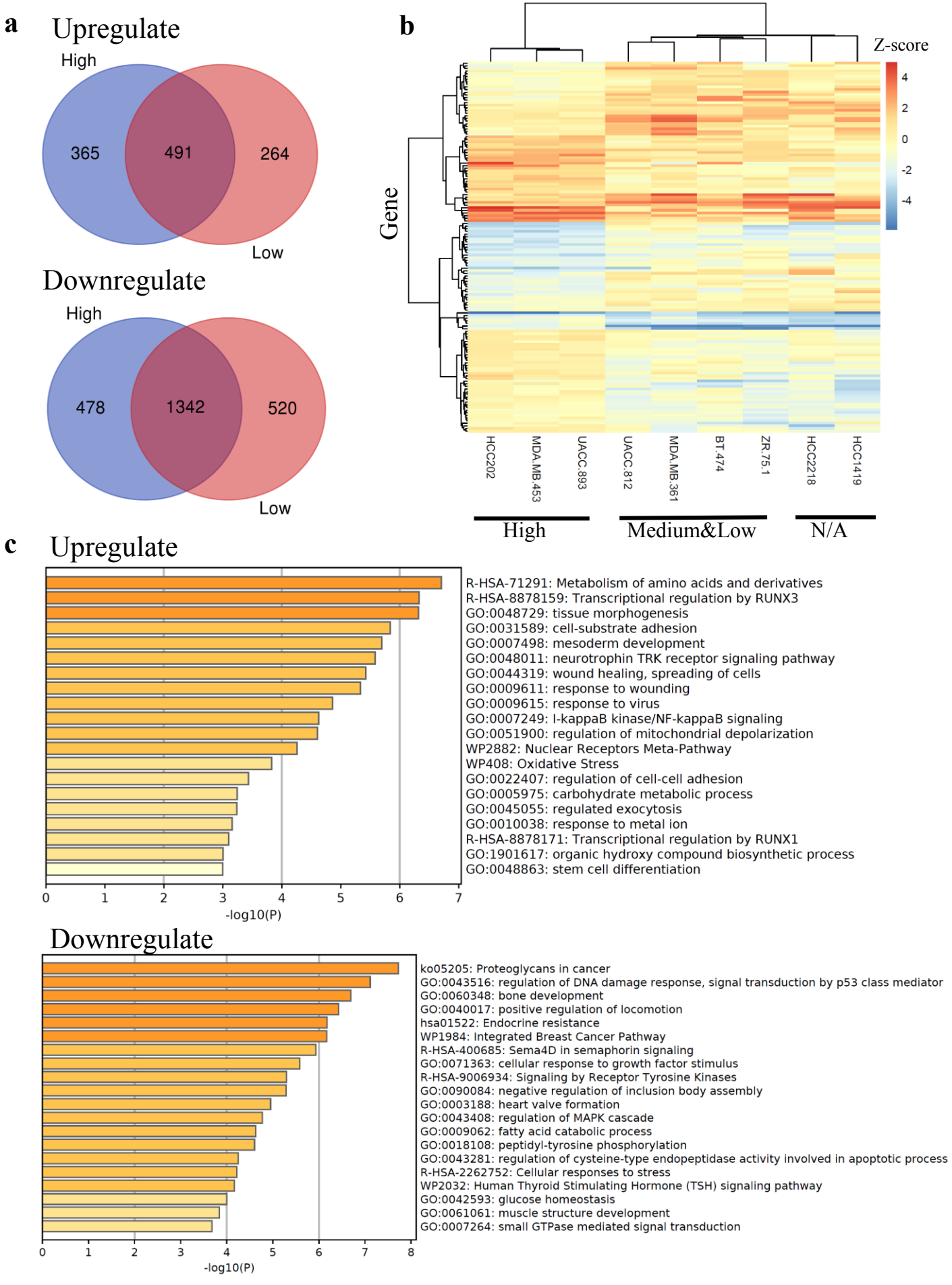
a
Upregulate
High
365
491
264
Low
Downregulate
High
478
1342
520
Low
b
Z-score
4
2
0
-2
-4
Gene
HCC202
MDA.MB.453
UACC.893
UACC.812
MDA.MB.361
BT.474
ZR.75.1
HCC2218
HCC1419
High
Medium&Low
N/A
c
Upregulate
R-HSA-71291: Metabolism of amino acids and derivatives
R-HSA-8878159: Transcriptional regulation by RUNX3
GO:0048729: tissue morphogenesis
GO:0031589: cell-substrate adhesion
GO:0007498: mesoderm development
GO:0048011: neurotrophin TRK receptor signaling pathway
GO:0044319: wound healing, spreading of cells
GO:0009611: response to wounding
GO:0009615: response to virus
GO:0007249: I-kappaB kinase/NF-kappaB signaling
GO:0051900: regulation of mitochondrial depolarization
WP2882: Nuclear Receptors Meta-Pathway
WP408: Oxidative Stress
GO:0022407: regulation of cell-cell adhesion
GO:0005975: carbohydrate metabolic process
GO:0045055: regulated exocytosis
GO:0010038: response to metal ion
R-HSA-8878171: Transcriptional regulation by RUNX1
GO:1901617: organic hydroxy compound biosynthetic process
GO:0048863: stem cell differentiation
0
1
2
3
4
5
6
7
-log10(P)
Downregulate
ko05205: Proteoglycans in cancer
GO:0043516: regulation of DNA damage response, signal transduction by p53 class mediator
GO:0060348: bone development
GO:0040017: positive regulation of locomotion
hsa01522: Endocrine resistance
WP1984: Integrated Breast Cancer Pathway
R-HSA-400685: Sema4D in semaphorin signaling
GO:0071363: cellular response to growth factor stimulus
R-HSA-9006934: Signaling by Receptor Tyrosine Kinases
GO:0090084: negative regulation of inclusion body assembly
GO:0003188: heart valve formation
GO:0043408: regulation of MAPK cascade
GO:0009062: fatty acid catabolic process
GO:0018108: peptidyl-tyrosine phosphorylation
GO:0043281: regulation of cysteine-type endopeptidase activity involved in apoptotic process
R-HSA-2262752: Cellular responses to stress
WP2032: Human Thyroid Stimulating Hormone (TSH) signaling pathway
GO:0042593: glucose homeostasis
GO:0061061: muscle structure development
GO:0007264: small GTPase mediated signal transduction
0
1
2
3
4
5
6
7
8
-log10(P)

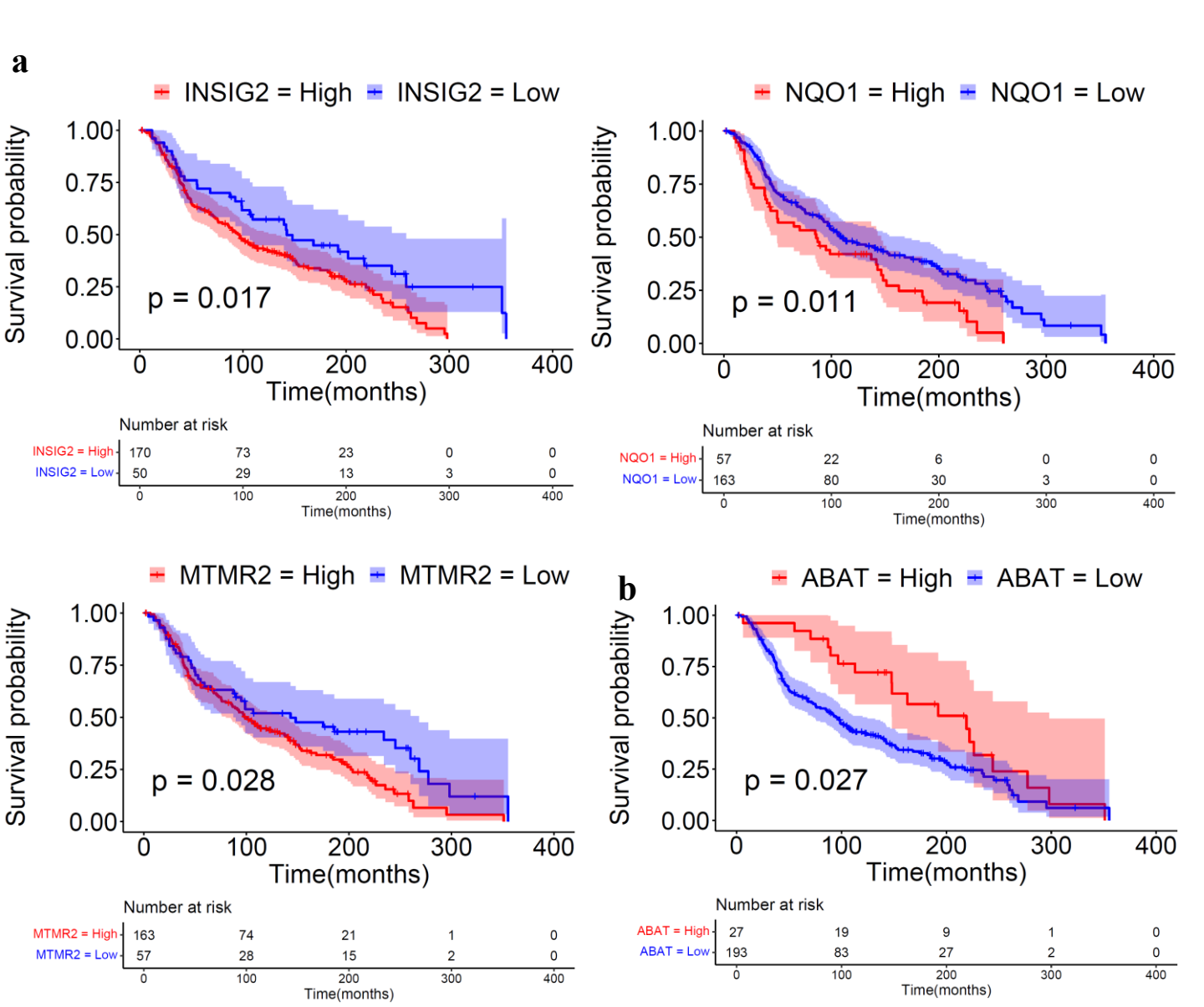
a
INSIG2 = High
INSIG2 = Low
Survival probability
1.00
0.75
0.50
0.25
0.00
p = 0.017
0
100
200
300
400
Time(months)
Number at risk
INSIG2 = High 170 73 23 0 0
INSIG2 = Low 50 29 13 3 0
NQO1 = High
NQO1 = Low
p = 0.011
NQO1 = High 57 22 6 0 0
NQO1 = Low 163 80 30 3 0
MTMR2 = High
MTMR2 = Low
p = 0.028
MTMR2 = High 163 74 21 1 0
MTMR2 = Low 57 28 15 2 0
b
ABAT = High
ABAT = Low
p = 0.027
ABAT = High 27 19 9 1 0
ABAT = Low 193 83 27 2 0

Figure 4

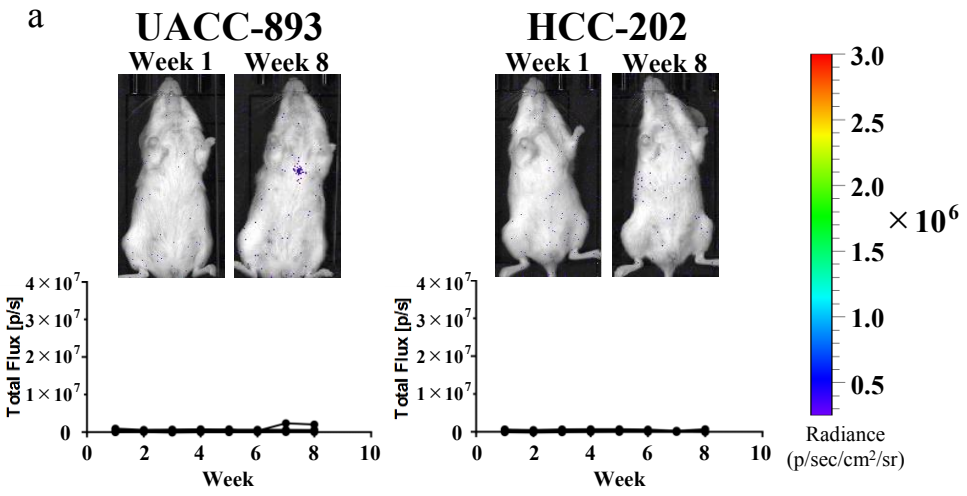
a
UACC-893
Week 1
Week 8
HCC-202
Week 1
Week 8
Total Flux [p/s]
Week
3.0
2.5
2.0
× 10^6
1.5
1.0
0.5
Radiance
(p/sec/cm²/sr)

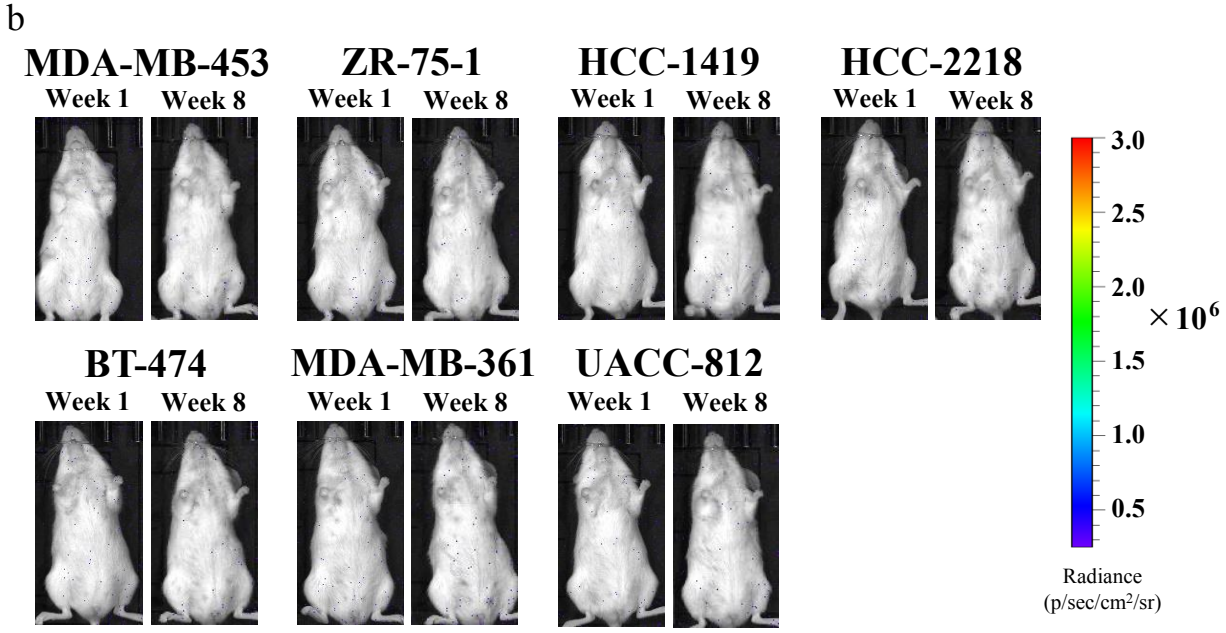
b
MDA-MB-453
ZR-75-1
HCC-1419
HCC-2218
BT-474
MDA-MB-361
UACC-812
Week 1
Week 8
3.0
2.5
2.0
× 10^6
1.5
1.0
0.5
Radiance
(p/sec/cm²/sr)

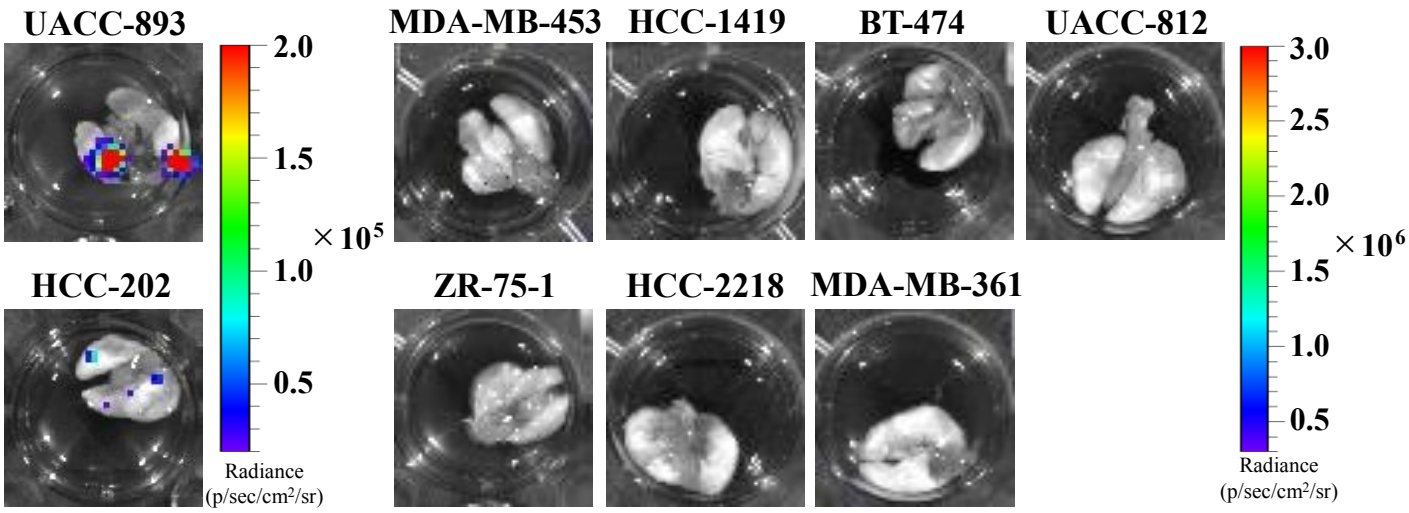
c
ex vivo Imaging of Lung
UACC-893
MDA-MB-453
HCC-1419
BT-474
UACC-812
HCC-202
ZR-75-1
HCC-2218
MDA-MB-361
2.0
1.5
× 10^5
1.0
0.5
Radiance
(p/sec/cm²/sr)
3.0
2.5
2.0
× 10^6
1.5
1.0
0.5
Radiance
(p/sec/cm²/sr)

a

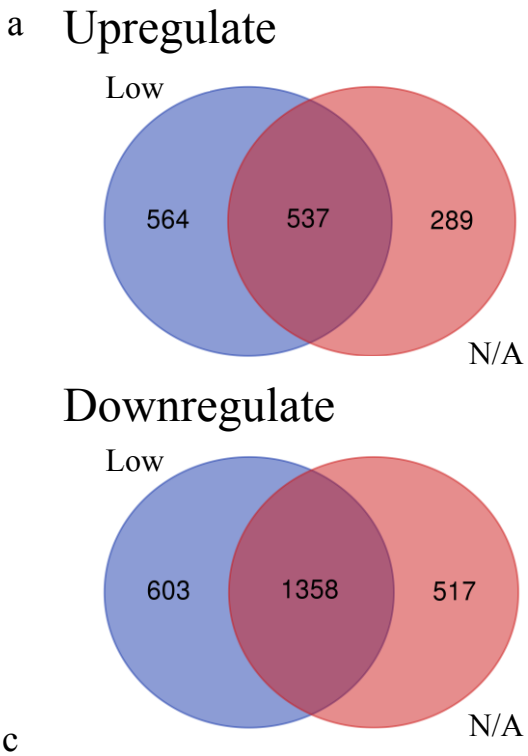

b

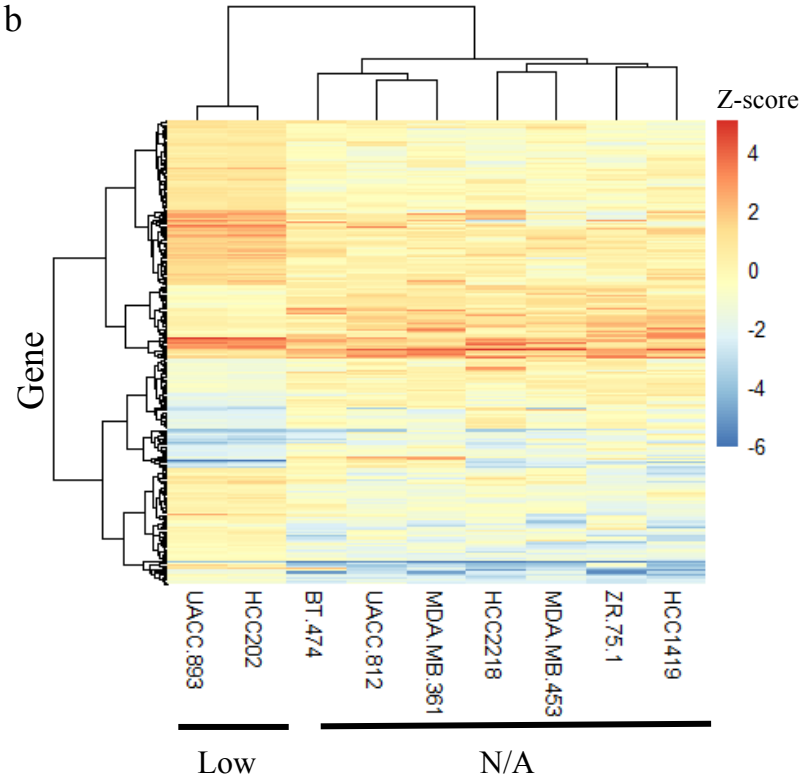

c

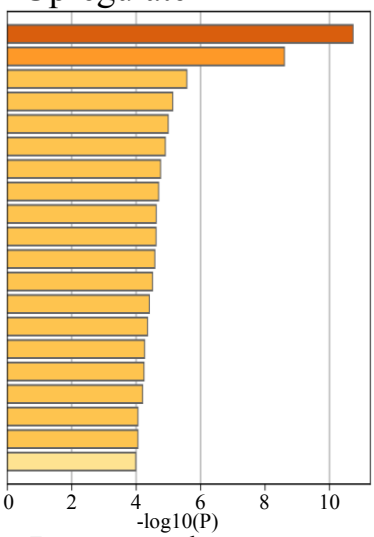

R-HSA-556833: Metabolism of lipids
WP2882: Nuclear receptors meta-pathway
R-HSA-8978868: Fatty acid metabolism
GO:0071417: cellular response to organonitrogen compound
hsa04916: Melanogenesis
R-HSA-382551: Transport of small molecules
WP2873: Aryl hydrocarbon receptor pathway
GO:0014075: response to amine
GO:0030855: epithelial cell differentiation
GO:0042493: response to drug
R-HSA-3928665: EPH-ephrin mediated repulsion of cells
R-HSA-8862803: Deregulated CDK5 triggers multiple neurodegenerative pathways in Alzheimer's disease models
GO:0009611: response to wounding
GO:0000578: embryonic axis specification
GO:0006914: autophagy
GO:0007420: brain development
GO:1901615: organic hydroxy compound metabolic process
GO:0006820: anion transport
GO:0035235: ionotropic glutamate receptor signaling pathway
GO:1903727: positive regulation of phospholipid metabolic process

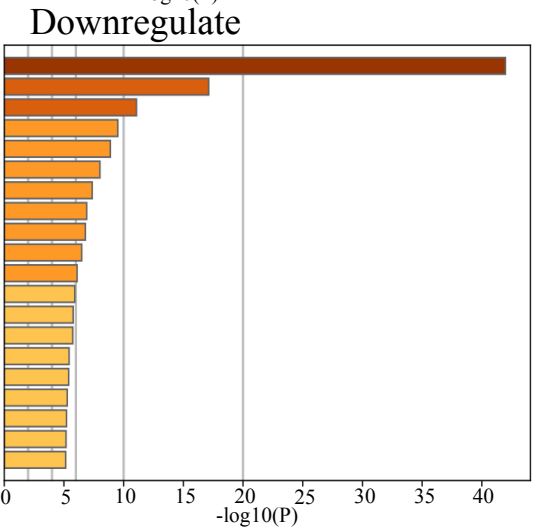

R-HSA-156842: Eukaryotic Translation Elongation
GO:1903047: mitotic cell cycle process
R-HSA-1640170: Cell Cycle
GO:0022613: ribonucleoprotein complex biogenesis
GO:0044770: cell cycle phase transition
R-HSA-109582: Hemostasis
R-HSA-72203: Processing of Capped Intron-Containing Pre-mRNA
GO:0007420: brain development
ko03013: RNA transport
GO:0051640: organelle localization
GO:0008285: negative regulation of cell population proliferation
GO:0000904: cell morphogenesis involved in differentiation
GO:0046649: lymphocyte activation
WP289: Myometrial relaxation and contraction pathways
GO:1903320: regulation of protein modification by small protein conjugation or removal
GO:0061351: neural precursor cell proliferation
R-HSA-2980766: Nuclear Envelope Breakdown
GO:0051129: negative regulation of cellular component organization
GO:0033044: regulation of chromosome organization
M14: PID AURORA B PATHWAY

a

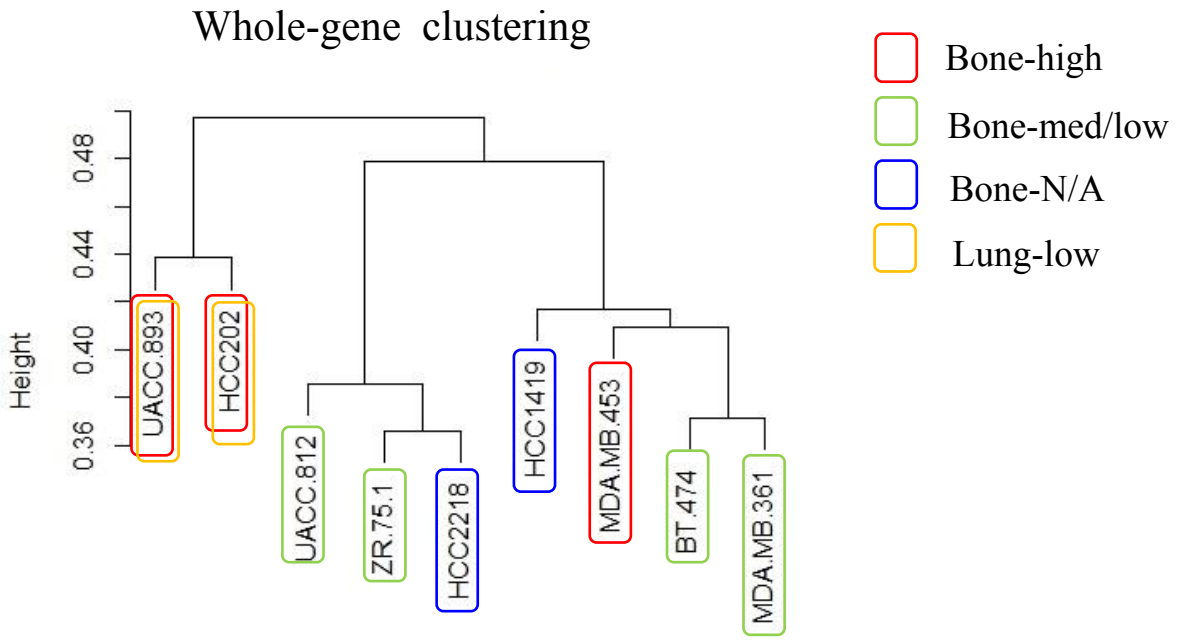
Whole-gene clustering
Bone-high
Bone-med/low
Bone-N/A
Lung-low
Height
0.36
0.40
0.44
0.48
UACC.893
HCC202
UACC.812
ZR.75.1
HCC2218
HCC1419
MDA.MB.453
BT.474
MDA.MB.361

b

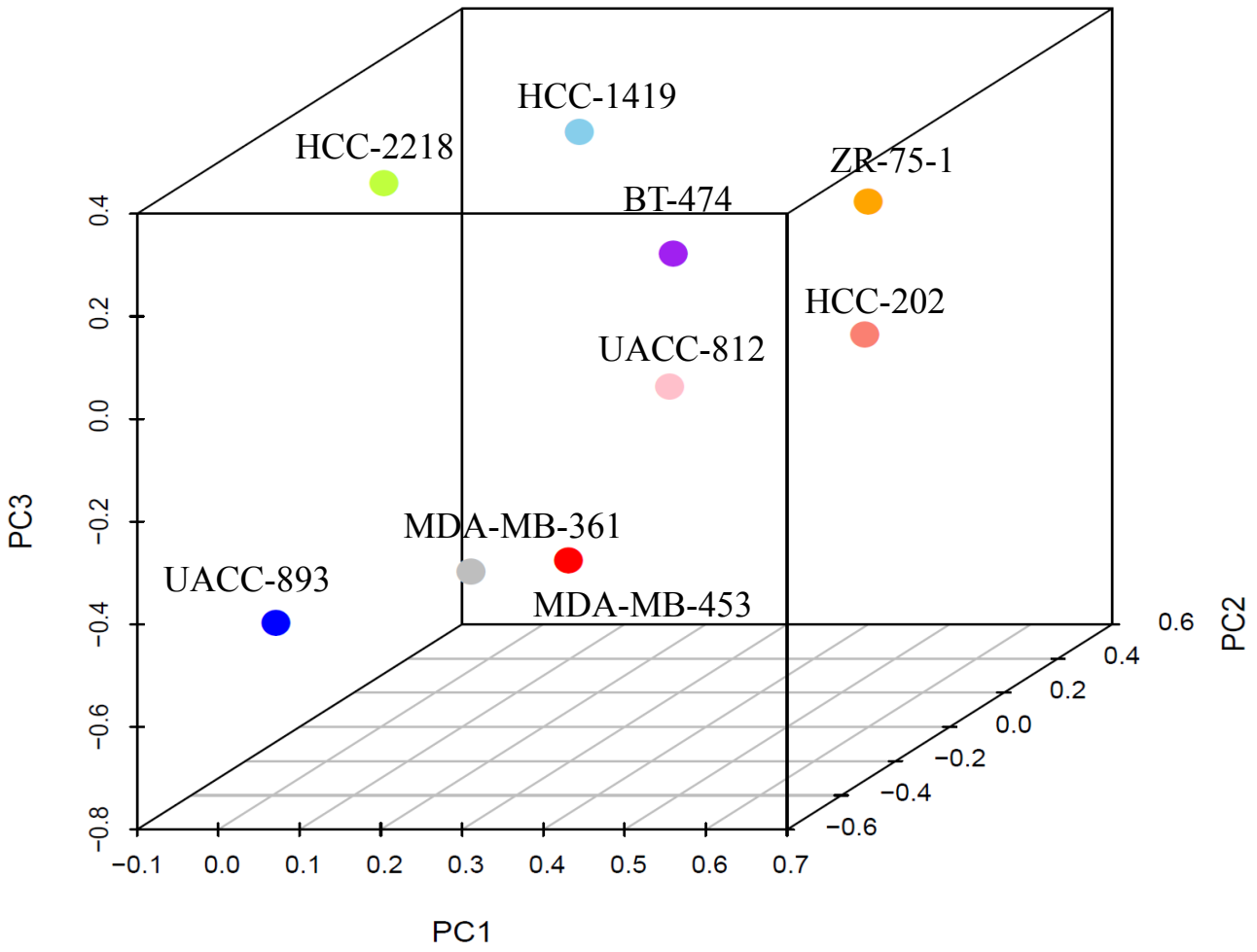
HCC-1419
HCC-2218
ZR-75-1
BT-474
HCC-202
UACC-812
MDA-MB-361
UACC-893
MDA-MB-453
PC3
0.4
0.2
0.0
−0.2
−0.4
−0.6
−0.8
PC1
−0.1
0.0
0.1
0.2
0.3
0.4
0.5
0.6
0.7
PC2
0.6
0.4
0.2
0.0
−0.2
−0.4
−0.6

Upregulate

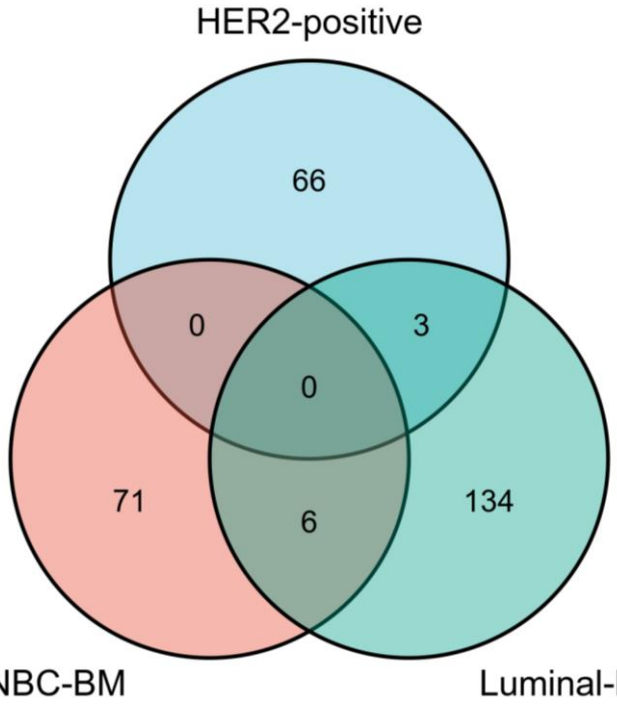

HER2-positive AND Luminal-BM NOT TNBC-BM	TNBC-BM AND Luminal-BM NOT HER2-positive
LGALS1	AGR2
FLNA	CYFIP2
ASPH	DUSP13
	RORA
	S100A4
	SERPINF1

Downregulate

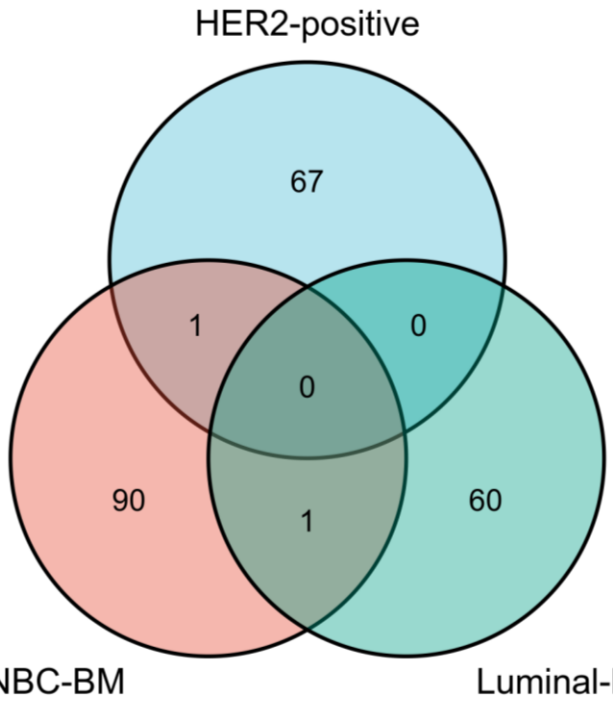

HER2-positive AND TNBC-BM NOT Luminal-BM	TNBC-BM AND Luminal-BM NOT HER2-positive
ADAMTS15	ADAMTS19

Upregulate

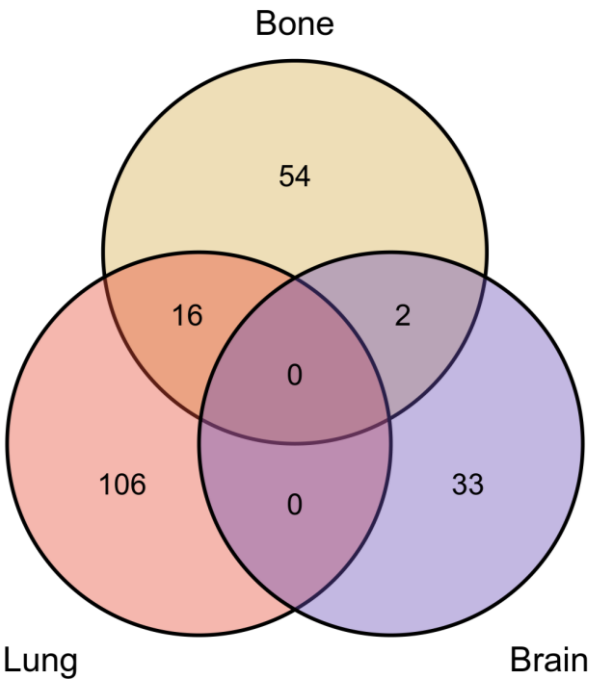

Downregulate

Bone AND Lung NOT Brain	Bone AND Brain NOT Lung
ALG8	LGALS1
SPRY1	INHBB2
ACP1	
DDIT4	
NQO1	
JUB	
TEAD2	
ODC1	
INSIG2	
MTMR2	
EXT1	
CKLF	
TXNRD1	
DKFZp762C186	
TACSTD2	
FLOT1	

Bone AND Lung NOT Brain	Bone AND Brain NOT Lung	Lung AND Brain NOT Bone	Bone AND Lung AND Brain
ZNF385	FOXD1	RBBP7	MYBL1
RPL9	CTTNBP2	ARSD	ABAT
GDF1	KREMEN1	PCSK1N	TWIST1
TGM2	FLJ23749	SCGB1D2	OLFM1
NAB1	IGF1R		
LARGE	TPBG		
RPL26	ESR1		
SCAM1	MGC4266		
ARHGDIG			
KCNG1			
PLP2			
TMEM16A			
ADAMTS15			
MPP6			
GNAS			
VIPR2			
PKIA			
FABP5			

Table 1. Metastasis profile of HER2-positive cell line

Cell line	Bone metastatic tumor number / total leg number	Bone metastasis ability evaluation	Lung metastatic tumor number / total mouse number	Lung metastasis ability evaluation
MDA-MB-453	3/8	High	0/9	N/A
UACC893	4/8	High	1/7	Low
HCC202	7/8	High	2/5	Low
BT474	3/8	Medium	0/4	N/A
ZR-75-1	4/8	Medium	0/4	N/A
MDA-MB-361	5/8	Low	0/3	N/A
UACC812	4/8	Low	0/4	N/A
HCC1419	0/8	N/A	0/4	N/A
HCC2218	0/8	N/A	0/4	N/A

Table 2. Top 30 upregulated DEGs of HER2-positive bone metastasis gene signatures

Gene_ name	Gene_ID	LogFC
GAGED2	NM_020411	3.981117
SECTM1	NM_003004	3.474067
SLCO2A1	NM_005630	2.83765
LGALS1	NM_002305	2.492867
IQGAP2	NM_006633	2.341167
CALML5	NM_017422	2.236683
TEAD2	NM_003598_(2)	2.21825
KMO	NM_003679	1.987383
G6PD	NM_000402	1.987317
INSIG2	NM_016133	1.936917
LOC51668	NM_016126	1.924967
INHBB	NM_002193	1.869333
ACN9	NM_020186	1.85965
CXorf6	NM_005491	1.8036
SQRDL	NM_021199	1.774333
TEAD2	NM_003598	1.7451
SYT12	NM_177963	1.679267
JUB	NM_198086	1.679033
COMMD3	NM_012071	1.6636
FLNA	NM_001456	1.61915
LGALS8	NM_201545	1.602083
PLEKHC1	NM_006832	1.5816
APOBEC3B	NM_004900	1.573883
JUB	NM_032876	1.555883
CYBRD1	NM_024843	1.55275
MEST	NM_002402	1.544767
DKFZp762C186	XM_170658	1.517167
NQO1	NM_000903	1.5128
ODC1	NM_002539	1.50245
CKLF	NM_016951	1.464183

Table 3. Top 30 upregulated DEGs of HER2-positive lung metastasis gene signatures

Gene _name	Gene_ ID	LogFC
MAGEA2	NM_175743	4.4271
MAGEA9	NM_005365	3.6886
FADS2	NM_004265	3.6285
MESP1	NM_018670	3.4448
D2S448	XM_056455	3.1991
CDH3	NM_001793	2.934
TMPRSS2	NM_005656	2.8641
CRIM1	NM_016441	2.7695
PDE4B	NM_002600	2.5558
EDN1	NM_001955	2.5277
EFEMP1	NM_004105	2.4872
ABCC3	NM_003786	2.4322
PHYH	NM_006214	2.3426
FLJ22671	NM_024861_(2)	2.3006
LGALS1	NM_002305	2.2823
TEAD2	NM_003598_(2)	2.1974
MDS025	NM_021825	2.1381
TP53BP2	NM_005426_(2)	2.1045
PPARBP	NM_004774	2.0872
KIAA0644	AB014544	2.0859
UBE2L6	NM_004223	2.0311
PCP4	NM_006198	2.0165
ACN9	NM_020186	1.9784
CAPN2	NM_001748	1.9782
AK5	NM_012093	1.9767
JUB	NM_198086	1.8751
ASS	NM_000050	1.8692
TENS1	NM_022748	1.8676
STAT5A	NM_003152	1.8587
IBRDC2	NM_182757	1.856